GAS6 is a key homeostatic immunological regulator of host–commensal interactions in the oral mucosa

Maria Nassar[a], Yaara Tabib[a], Tal Capucha[a], Gabriel Mizraji[a], Tsipora Nir[a], Meirav Pevsner-Fischer[b], Gili Zilberman-Schapira[b], Oded Heyman[c], Gabriel Nussbaum[a], Herve Bercovier[d], Asaf Wilensky[c], Eran Elinav[b], Tal Burstyn-Cohen[a,1,2], and Avi-Hai Hovav[a,1,2]

[a]Institute of Dental Sciences, Faculty of Dental Medicine, Hebrew University, Jerusalem 91120, Israel; [b]Department of Immunology, Weizmann Institute of Science, Rehovot 7610001, Israel; [c]Department of Periodontology, Faculty of Dental Medicine, Hadassah Medical Center, Jerusalem 91120, Israel; and [d]Department of Microbiology and Molecular Genetics, Faculty of Medicine, Hebrew University, Jerusalem 91120, Israel

Edited by Lora V. Hooper, University of Texas Southwestern, Dallas, TX, and approved December 7, 2016 (received for review September 6, 2016)

The oral epithelium contributes to innate immunity and oral mucosal homeostasis, which is critical for preventing local inflammation and the associated adverse systemic conditions. Nevertheless, the mechanisms by which the oral epithelium maintains homeostasis are poorly understood. Here, we studied the role of growth arrest specific 6 (GAS6), a ligand of the TYRO3–AXL–MERTK (TAM) receptor family, in regulating oral mucosal homeostasis. Expression of GAS6 was restricted to the outer layers of the oral epithelium. In contrast to protein S, the other TAM ligand, which was constitutively expressed postnatally, expression of GAS6 initiated only 3–4 wk after birth. Further analysis revealed that GAS6 expression was induced by the oral microbiota in a myeloid differentiation primary response gene 88 (MyD88)-dependent fashion. Mice lacking GAS6 presented higher levels of inflammatory cytokines, elevated frequencies of neutrophils, and up-regulated activity of enzymes, generating reactive nitrogen species. We also found an imbalance in Th17/Treg ratio known to control tissue homeostasis, as Gas6-deficient dendritic cells preferentially secreted IL-6 and induced Th17 cells. As a result of this immunological shift, a significant microbial dysbiosis was observed in *Gas6*$^{-/-}$ mice, because anaerobic bacteria largely expanded by using inflammatory byproducts for anaerobic respiration. Using chimeric mice, we found a critical role for GAS6 in epithelial cells in maintaining oral homeostasis, whereas its absence in hematopoietic cells synergized the level of dysbiosis. We thus propose GAS6 as a key immunological regulator of host–commensal interactions in the oral epithelium.

oral mucosa | GAS6 | TAM | homeostasis | microbiota

The stratified epithelium covering the oral mucosa is continuously challenged by an immense amount of diverse microorganisms, some of which might be pathogenic. Emerging evidence suggests that mucosal epithelial cells in simple epithelial tissues, such as in the intestine and lung, are an essential component of a communications network. As such, they transmit and receive signals from cells in the underlying mucosal layers, which are critical to coordinate homeostatic and inflammatory functions (1, 2). Oral epithelial cells were also found to respond to various microbial challenges and to produce proinflammatory and antimicrobial molecules (3, 4). Therefore, the stratified oral epithelium not only forms a physical barrier to oral microorganisms, but actively participates in inducing immunity, thus providing an immunological barrier. Nevertheless, whereas much attention was given in recent years to study oral mucosal immunity in a setting of infection or immunization, less attention was given to mechanisms engaged by the oral mucosa to maintain homeostasis. Perhaps the most challenging role in this regard is the task of the gingival epithelium, which monitors biofilm development on the tooth surface. The teeth represent the only hard tissue in our body exposed to the hostile external environment, and bacteria colonize tooth enamel and adjacent soft tissues to form a persistent and chronic biofilm (5). An excessive inflammatory response against the oral biofilm results in periodontal diseases, and can facilitate intravascular dissemination of microorganisms throughout the body that is associated with adverse systemic conditions (6). Therefore, understanding the immune mechanisms engaged by the oral mucosal epithelium to maintain immunological homeostasis is of major importance for human health.

Maintaining immune homeostasis is an active and complex process requiring vast interplays among hematopoietic and nonhematopoietic cells such as epithelial cells. Recently, the TAM receptors: TYRO3, AXL, and MERTK and their ligands: growth arrest-specific 6 (GAS6) and protein S (PROS1) were shown to play a critical role in the resolution of inflammation (7). This is achieved by the ability of TAM signaling to down-regulate innate inflammatory responses, mediate efferocytosis, and restore vascular integrity (8). Despite the high structural homology between GAS6 and PROS1, both ligands have distinct affinities to the TAM receptors and are also differentially expressed in various cell types (9). Furthermore, whereas the functions of GAS6 seem to be limited to those caused by activation of the TAM receptors, PROS1 has TAM receptor-dependent and independent activities (8, 10–12). In line with their discrete properties, GAS6 and PROS1 were shown to control distinct immune mechanisms in vitro and in vivo (7).

Due to the aforementioned function of TAM signaling, we envisaged that TAM receptors and their cognate ligands might be expressed in the oral mucosa and could play a role in regulating mucosal immunity. Indeed, we revealed that expression of

Significance

Understanding the mechanisms by which the immune system and local microorganisms coexist in the oral cavity is important, as disruption of this delicate balance could cause oral and systemic diseases. We revealed that growth arrest specific 6 (GAS6), a ligand of the TYRO3–AXL–MERTK signaling system, plays a critical role in this process. Upon birth, microorganisms residing in the oral cavity induce expression of GAS6 in oral tissues; GAS6 in turn regulates antibacterial function in these tissues. We also found that GAS6 expressed by cells of the immune system further contributes to its regulatory role in oral tissues. Collectively, this work proposes that GAS6 restrains the immune response in the oral cavity to maintain coexistence with favorable microorganisms residing within the oral cavity.

Author contributions: H.B., A.W., T.B.-C., and A.-H.H. designed research; M.N., Y.T., G.M., T.N., O.H., and A.W. performed research; G.N. and E.E. contributed new reagents/analytic tools; M.N., T.C., M.P.-F., G.Z.-S., O.H., and E.E. analyzed data; and T.B.-C. and A.-H.H. wrote the paper.

The authors declare no conflict of interest.

This article is a PNAS Direct Submission.

[1]T.B.-C. and A.-H.H. contributed equally to this work.

[2]To whom correspondence may be addressed. Email: avihaih@ekmd.huji.ac.il or talbu@ekmd.huji.ac.il.

This article contains supporting information online at www.pnas.org/lookup/suppl/doi:10.1073/pnas.1614926114/-/DCSupplemental.

GAS6 in the oral epithelium is induced by oral microbiota and plays a critical role in maintaining immunological and microbial oral homeostasis. We thus propose a fundamental role for GAS6 in regulating host–commensal interactions in the oral mucosa.

Results

Expression of GAS6 and PROS1 in the Oral Mucosa. We first sought to characterize expression of the two TAM ligands in the oral mucosa. The gingiva represents the tissue surrounding and monitoring the oral biofilm (Fig. S1*A*), and thus we analyzed expression of these ligands in gingival cross-sections. Expression of GAS6 and PROS1 was mainly observed in the gingival epithelium, as demonstrated by immunofluorescence, real-time PCR and Western blot analyses (Fig. 1*A* and Fig. S1 *B* and *C*). Within the epithelium, GAS6 was detected only in the most peripheral epithelial layers, whereas PROS1 was also expressed in deeper layers of the epithelium. In line with these observations, colocalization of both ligands was observed in the external layers of the epithelium (Fig. 1*A*, *iv*). Importantly, similar expression patterns of GAS6 and PROS1 were also observed in human gingival tissues (Fig. 1*B*). Because the gingiva is not completely developed until the teeth are erupted, a process occurring in mice between the second and third weeks of life, we next assessed expression kinetics from birth to adulthood. As depicted in Fig. 1*C*, GAS6 and PROS1 displayed distinct expression dynamics. Whereas PROS1 was constitutively expressed after birth, GAS6 was detected in the epithelium only after the teeth eruption, ∼3–4 wk after birth. Studies have shown that among the three TAM receptors, GAS6 binds to AXL with highest affinity in vivo (13), thus we next assessed expression of AXL in the gingiva. Similar to GAS6 expression, AXL was mainly expressed in the peripheral layers of the oral epithelium (Fig. 1*D* and Fig. S1*D*). Taken together, our data demonstrate that whereas both TAM ligands, GAS6 and PROS1, are expressed in the oral epithelium, they have distinct kinetics and pattern of expression in mice and also in human. Furthermore, the similar expression pattern of AXL and GAS6 in the epithelium suggests that GAS6 might act via AXL in the oral mucosa.

Expression of GAS6 in the Epithelium Is Induced by Oral Commensals. During the first weeks after birth, the murine oral microbiota undergoes dramatic changes, as the mice are weaned and the biofilm starts to develop on the newly erupted teeth (14). We thus hypothesized that expression of GAS6 in the oral epithelium

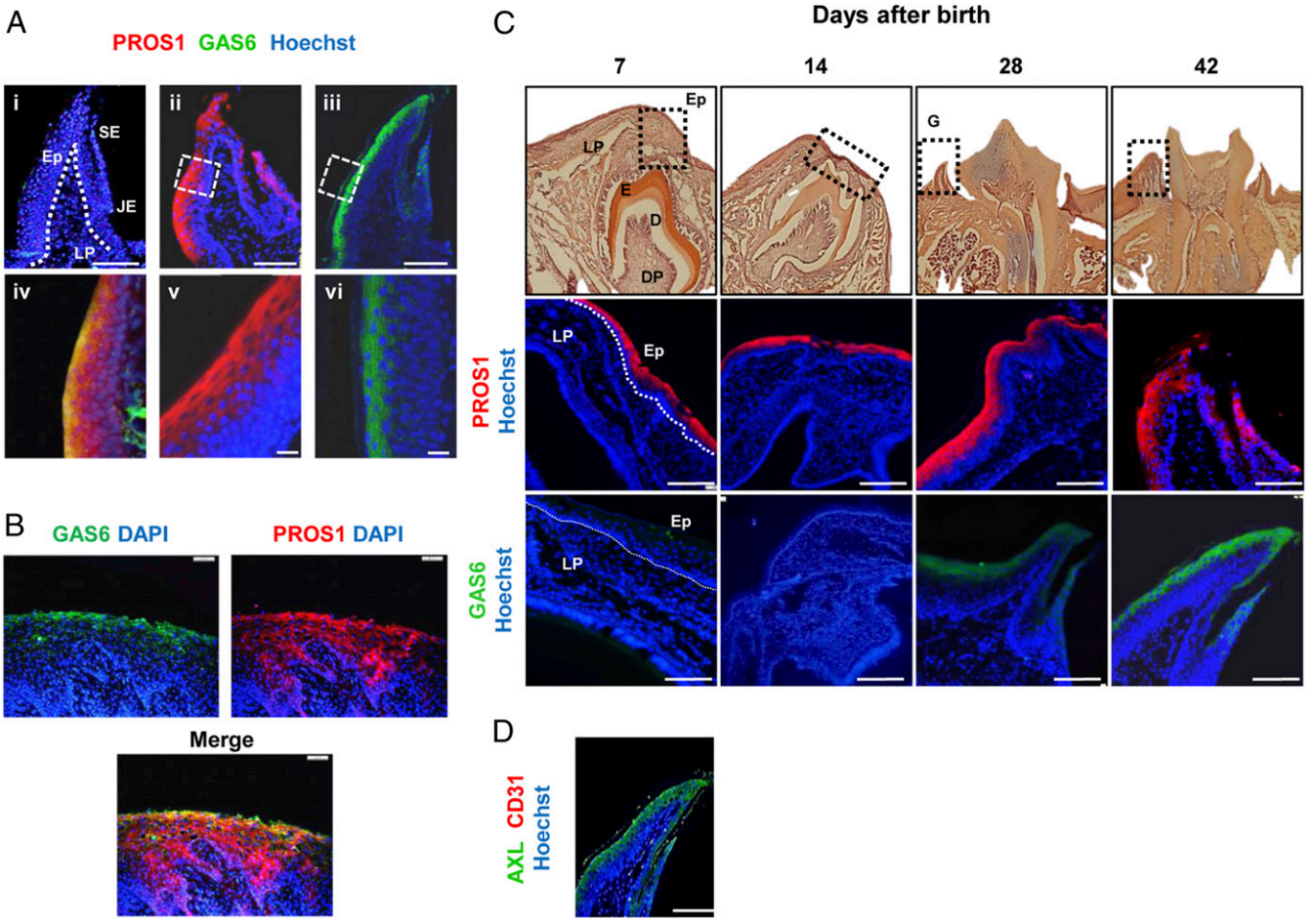

Fig. 1. Expression profiles of GAS6, PROS1, and AXL in the oral mucosa. (*A*) Gingival cross-sections of adult B6 mice were stained with antibodies against GAS6 (green), PROS1 (red), and Hoechst (nuclei, blue) for immunofluorescence analysis. (*i*) No primary antibody control, (*ii* and *v*) PROS1, (*iii* and *vi*) GAS6, and (*iv*) colocalization of GAS6 and PROS1. Representative images of at least six independent experiments are shown. (Scale bars, 50 μm.) (*B*) Gingival cross-sections of human gingival tissues were stained with antibodies against GAS6 (green), PROS1 (red), and DAPI (nuclei, blue) for immunofluorescence analysis. (Scale bars, 200 μm.) (*C*) Gingival tissues were harvested at different time points after birth for H&E and immunofluorescence analysis: PROS1 (red), GAS6 (green), and Hoechst (blue). Representative images of two independent experiments are shown ($n = 12$). (Scale bars, 50 μm.) (*D*) Immunofluorescence analysis of gingival cross-sections of adult B6 mice stained with antibodies against AXL (green) and Hoechst (nuclei, blue). Representative images of at least five independent experiments are shown ($n = 10$). (Scale bars, 50 μm.) Ep, epithelium; LP, lamina propria; SE, sulcular epithelium; JE, junctional epithelium. E, enamel; D, dentin; and DP, dental papilla.

might be induced by such microbial changes. To address this issue, we examined expression of GAS6 in the gingival epithelium of germ-free (GF) mice by immunofluorescence and RT-quantitative PCR (RT-qPCR). Age- and sex-matched adult male Swiss Webster mice housed under GF or specific pathogen-free (SPF) conditions were analyzed. In contrast to SPF mice, GAS6 was not expressed in the gingiva of GF mice (Fig. 2 *A* and *B*). Colonization of GF mice with bacteria following cocaging with SPF mice for 2 mo restored GAS6 expression, though not to similar levels as in SPF mice. We next assessed expression of PROS1 in GF mice and found that PROS1 was not significantly altered by bacterial colonization in these mice. Similarly, expression of AXL was not affected by the presence or absence of the oral microbiota (Fig. 2 *A* and *B*). To examine whether the induction of GAS6 expression by oral bacteria involves recognition via Toll-like receptor (TLR) signaling, we analyzed mice lacking myeloid differentiation primary response gene 88 (MyD88), a molecule mediating intracellular signaling of most TLRs. As demonstrated in Fig. 2*C*, GAS6 expression was abolished in *Myd88*$^{-/-}$ mice that were house in SPF conditions, as demonstrated by immunofluorescence and RT-qPCR analyses. These data suggest that oral microbiota induces expression of GAS6 in the gingival epithelium in a MYD88-dependent signaling pathway.

GAS6 Regulates Oral Mucosal Immunity at Steady State. Induction of GAS6 expression in the epithelium by oral microbiota might indicate that GAS6 regulates mucosal immune responses to the colonizing bacteria. We thus examined how the absence of GAS6 impacts oral mucosal immunity in *Gas6*$^{+/+}$ and *Gas6*$^{-/-}$ littermate controls. Using flow cytometry analysis (gating strategies are provided in Fig. S2*A*), we first found similar numbers of total leukocytes, T and B lymphocytes in the gingiva of adult *Gas6*$^{-/-}$ and *Gas6*$^{+/+}$ mice maintained under SPF conditions (Fig. 3*A*). Nevertheless, compared with *Gas6*$^{+/+}$ mice, *Gas6*$^{-/-}$ mice have elevated numbers of neutrophils (CD45^{+}CD11b^{+}Ly6G^{+} cells) (Fig. 3*A*). A significant increase in the frequencies of gingival dendritic cells (DCs) (CD45^{+}CD11c^{+}MHCII^{+} cells) was also detected in *Gas6*$^{-/-}$ mice. However, their activation state, based on MHCII and CD86 expression levels, was not significantly altered due to the absence of GAS6 (Fig. 3*B* and Fig. S2*B*). We next focused our analysis on T regulatory (Treg) and Th17 cells, which are known to have a critical role in tissue homeostasis (15). As illustrated in Fig. 3*C*, the frequencies of FOXP3^{+} CD4^{+} T cells were significantly higher in the gingiva of *Gas6*$^{+/+}$ in comparison with *Gas6*$^{-/-}$ mice. Using RT-qPCR, we also found elevated levels of *Foxp3* mRNA in the gingiva of *Gas6*$^{+/+}$ relative to *Gas6*$^{-/-}$ mice. We then quantified mRNA levels of IL-10 and TNF-α in the gingiva, and concurring with our results, IL-10 was highly expressed in *Gas6*$^{+/+}$ mice, whereas TNF-α was predominantly expressed in *Gas6*$^{-/-}$ mice (Fig. 3*C*). To quantify the frequencies of Th17 in the gingiva, gingival cells were isolated, stimulated with phorbol 12-myristate 13-acetate (PMA)/ionomycin and IL-17A^{+} CD4^{+} T cells were identified by intracellular cytokine staining (ICS). As demonstrated in Fig. 3*D*, the gingiva of *Gas6*$^{-/-}$ mice contained significantly higher percentages of IL-17A-producing CD4^{+} T cells than *Gas6*$^{+/+}$ mice. Furthermore, the amount of IL-17A per cell was higher in gingival CD4^{+} T cells of *Gas6*$^{-/-}$ compared with *Gas6*$^{+/+}$ mice. In line with these findings, we also found in the gingiva of *Gas6*$^{-/-}$ mice higher levels of IL-17A and IFN-α mRNA, the latter known, even at low expression levels, to shape tonic signals by modulating cytokine expression and therefore regulating tissue homeostasis (Fig. 3 *E* and *F*) (16). Collectively, these results indicate that the lack of GAS6 resulted in an increased inflammatory milieu in the oral mucosa.

***Gas6*$^{-/-}$ DCs Preferentially Induce Th17 Rather than Treg Cells.** As T-cell polarization is executed by DCs, we next analyzed the impact of GAS6 on the capacity of DCs to stimulate T cells. First, we examined whether GAS6 is expressed in DCs by performing immunofluorescence analysis on MHCII^{high}CD11c^{+} cells sorted from the oral mucosa-draining lymph nodes (LNs) of *Gas6*$^{+/+}$ mice. GAS6 was clearly identified in DCs, and appeared to colocalize with the MHCII molecule in the cytoplasm (Fig. 4*A*). The presence of GAS6 in DCs was also found in bone-marrow–generated DCs (BMDCs) using RT-qPCR and Western blot analyses (Fig. 4 *B* and *C*). Expression of GAS6 as well as its receptor AXL were up-regulated in BDMCs upon stimulation with LPS (Fig. 4 *B* and *C*). Furthermore, stimulated *Gas6*$^{-/-}$ BMDCs secreted higher levels of IL-6 compared with *Gas6*$^{+/+}$ BMDCs, a cytokine known to be involved in Th17/Treg polarization (Fig. 4*D*). Such secretion was able to promote ex vivo the differentiation of naive OT-II CD4^{+} T cells into IL-17A secreting cells upon coculturing and stimulation with LPS and the OVA$_{223–239}$ peptide (Fig. 4*E*).

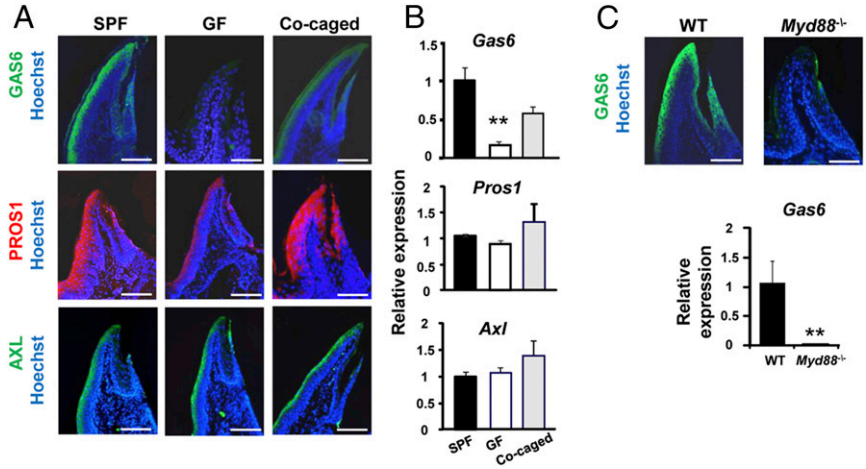

Fig. 2. GAS6 expression is induced by oral microbiota in a MYD88-dependent fashion. (*A*) Gingival cross-sections from adult Swiss Webster SPF mice, germ-free mice (GF), and GF mice cocaged with SPF mice for 2 mo, stained with antibodies against PROS1 (red), GAS6 (green), AXL (green), and Hoechst (blue). (Scale bars, 50 μm.) (*B*) RT-qPCR analysis quantifying expression of PROS1, GAS6, and AXL in the gingiva of the noted mice. Data indicate the relative expression levels of the noted gene among SPF, GF, and cocaged mice and represent the mean of five mice ± SEM. Representative data of one of two independent experiments are shown. (*C*) Gingival cross-sections from B6 and *Myd88*$^{-/-}$ mice stained with antibody against GAS6 (green) and Hoechst (blue). (Scale bars, 50 μm.) Bar graph illustrates levels of *Gas6* expression in B6 and *Myd88*$^{-/-}$ mice and represent the mean of three mice ± SEM. Representative data of one of two independent experiments are shown.

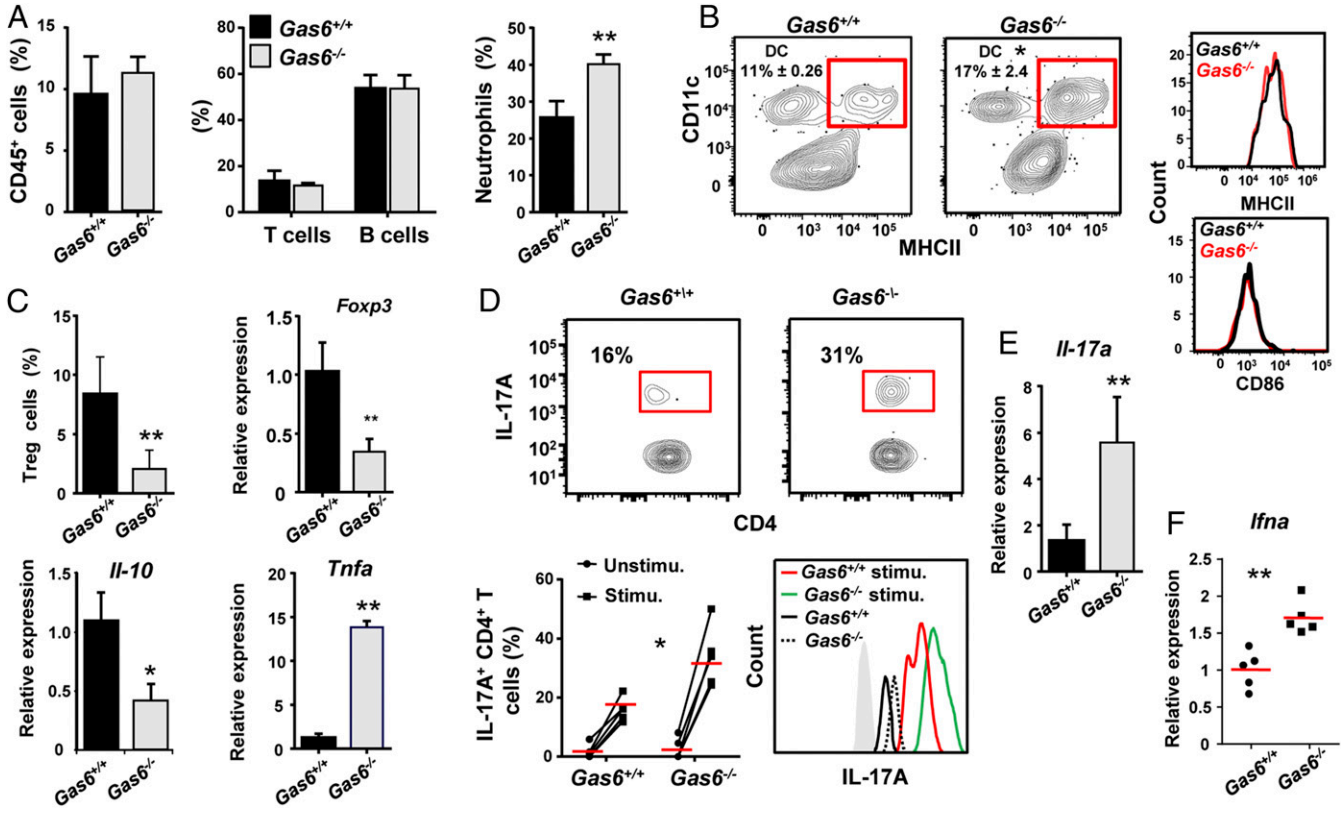

Fig. 3. Elevated inflammatory milieu in the gingiva of *Gas6*$^{-/-}$ mice at steady state. (*A*–*C*) Gingival tissues of adult naive *Gas6*$^{+/+}$ and *Gas6*$^{-/-}$ littermate controls were processed and analyzed by flow cytometry. (*A*) Frequencies of total CD45^{+} leukocytes, T and B lymphocytes, and neutrophils. (*B*, *Left*) Representative FACS plots demonstrating the presence of DCs (CD11c^{+}MHCII^{+}) in the gingiva of each group; numbers indicate the percentages of DCs from CD45^{+} cells. (*Right*) Representative histogram plots showing expression levels of MHCII and CD86 on DCs. (*C*) Frequencies of Treg cells in the gingiva, and relative mRNA expression levels of *Foxp3*, *Il-10*, and *Tnf-a* quantified by RT-qPCR on total gingival tissues. Data represent the mean of five mice ± SEM. Representative data of one of three independent experiments are shown. (*D*) IL-17A expression produced in CD4^{+} T cells was determined by ICS from gingival cells prepared from naive and PMA/ionomycin-stimulated *Gas6*$^{+/+}$ and *Gas6*$^{-/-}$ mice. Representative FACS plots and graphs demonstrate the frequencies of IL-17A^{+} CD4^{+} T cells in *Gas6*$^{+/+}$ and *Gas6*$^{-/-}$ mice, as well as the intensity of IL-17A expression. Data represent the mean of five mice ± SEM. Representative data from one of three independent experiments are shown. (*E* and *F*) Bar graph depicts the relative mRNA levels of *Il-17a* (*E*) and *Ifna* (*F*) in the whole gingiva using RT-qPCR and represents the mean of five mice ± SEM. Representative data of one of three independent experiments are shown.

Because polarization of T cells occurs in the LNs by DCs migrating from the tissue, we analyzed Treg and Th17 cells in the oral-mucosa–draining LNs. Parallel to the gingiva, *Gas6*$^{-/-}$ mice have slightly reduced frequencies of Tregs in the LNs (Fig. 4*F*). Furthermore, the amount of FOXP3 expressed per cell was significantly reduced in *Gas6*$^{-/-}$ mice in comparison with *Gas6*$^{+/+}$ mice (Fig. 4*F*). Such a reduction in cellular FOXP3 levels was shown previously to severely impair Treg capability to regulate immunity (17). In contrast to Tregs, Th17 cells, identified by ICS on PMA/ionomycin-stimulated LN cells, were significantly higher in *Gas6*$^{-/-}$ mice compared with *Gas6*$^{+/+}$ mice (Fig. 4*G*). Akin to the gingiva, the amount of IL-17A per cell was considerably higher in *Gas6*$^{-/-}$ mice. Altogether, these data indicate that in the absence of GAS6, Treg/Th17 balance is skewed toward Th17 cells, leading to an increased inflammatory milieu in the oral mucosa at steady state. GAS6 thus plays a critical regulatory role in maintaining immunological homeostasis in the oral mucosa.

The Absence of GAS6 Alters the Load and Diversity of Oral Microbiota. We next sought to examine whether the absence of GAS6 would also have an impact on the oral microbiota. For this purpose, littermate controls of *Gas6*$^{+/+}$ and *Gas6*$^{-/-}$ mice were used. We first sampled bacteria using oral swabs from the oral cavity of individual age- and sex-matched *Gas6*$^{-/-}$ and *Gas6*$^{+/+}$ littermates born and housed under identical conditions. DNA was then extracted and the ratio of ribosomal 16S/18S genes was quantified to compare the microbial load in these mice. As demonstrated in Fig. 5*A*, the oral cavity of *Gas6*$^{-/-}$ mice sheltered an overall elevated bacterial load, about twofold higher, compared with *Gas6*$^{+/+}$ mice. We further compared the load of oral anaerobic bacteria in these mice, by plating oral swab samples on blood agar under anaerobic conditions. A considerable elevation of about 1.2 logs in the load of cultivated anaerobic bacteria was found in *Gas6*$^{-/-}$ mice in comparison with *Gas6*$^{+/+}$ mice (Fig. 5*B*). To test whether changes in the oral microbial load of *Gas6*$^{-/-}$ mice affects bacterial diversity, we performed a taxonomic analysis of the oral microbiota. As depicted in Fig. 5*C*, the absence of GAS6 led to a considerable shift in oral microbiota composition. Whereas the oral mucosa of *Gas6*$^{+/+}$ mice was mainly colonized by bacteria of the Firmicutes phylum, *Gas6*$^{-/-}$ mice contained three main phyla: Firmicutes, Proteobacteria, and Bacteriodetes. Moreover, the presence of *Streptococcaceae* (Firmicutes), representing the most common bacterial family in *Gas6*$^{+/+}$ mice, was drastically reduced in *Gas6*$^{-/-}$ mice, whereas other families of this phylum such as *Lactobacillaceae* and *Clostridiaceae*, were largely expanded (Fig. 5*C*). Alpha diversity analysis clearly confirmed the higher taxa richness in *Gas6*$^{-/-}$ mice compared with *Gas6*$^{+/+}$ mice ($P = 0.005$) (Fig. 5*D*). Moreover, the taxa present in these mice varied significantly as indicated by a weighted beta diversity and distance analyses (Fig. 5 *E* and *F*). We also tested Gas6$^{-/+}$ (heterozygous) mice for oral bacterial composition using specific primers against certain bacterial families largely altered in our system. Partial alterations of the examined bacterial families were

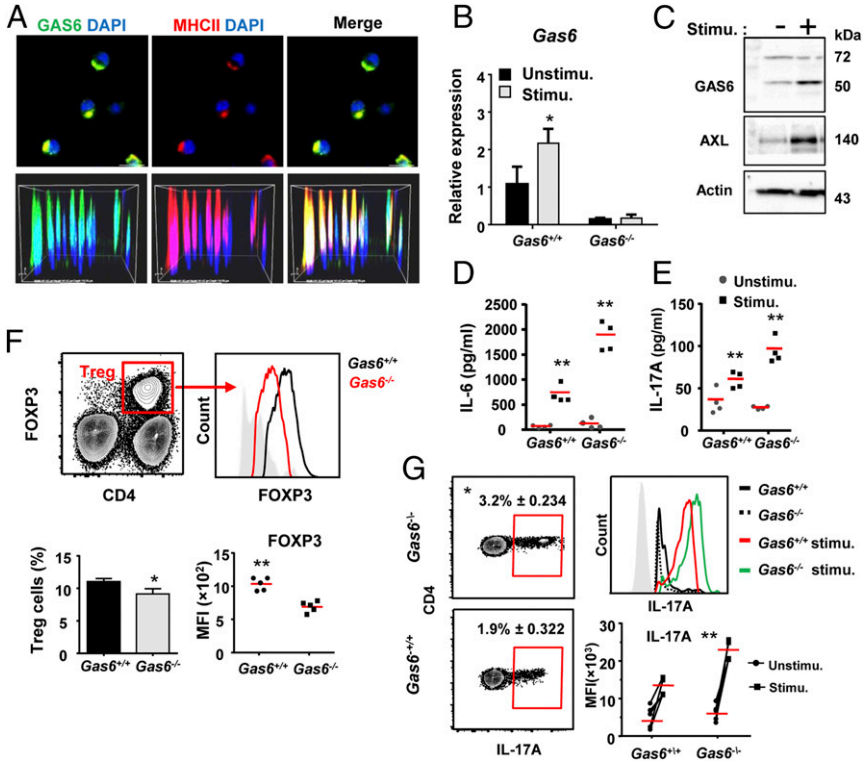

Fig. 4. Expression of GAS6 in DCs alters the polarization of Treg and Th17 cells. (*A*) Immunofluorescence analysis of DCs ($MHCII^+CD11c^+$ cells) sorted from cervical LNs of $Gas6^{+/+}$ mice, fixed on slides and stained with antibodies against GAS6 (green), MHCII (red), and Hoechst (blue). (Scale bar, 10 μm.) (*Lower*) Superimposed Z stacks of the stained DCs. (*B*) Quantification by RT-qPCR of GAS6 expression levels in BMDCs prepared from $Gas6^{+/+}$ and $Gas6^{-/-}$ mice stimulated or not with LPS. Data represent the mean of five mice per group ± SEM. Representative data of one of two independent experiments are shown. (*C*) Western blot analysis showing the presence of GAS6 and AXL in $Gas6^{+/+}$ BMDCs, either with or without LPS stimulation. (*D*) Concentration of IL-6 (quantified by ELISA) secreted by $Gas6^{+/+}$ or $Gas6^{-/-}$ BMDC cultured with or without LPS stimulation; data represent the mean of five replicates ± SEM. (*E*) IL-17A concentrations quantified by ELISA in the supernatant of $Gas6^{+/+}$ or $Gas6^{-/-}$ BDMCs cocultured with OT-II $CD4^+$ T cells and stimulated with LPS and $OVA_{223–239}$ peptide. Data represent the mean of five replicates ± SEM. Representative data of one of two to three independent experiments are shown. (*F*) Cervical LN cells were collected from $Gas6^{+/+}$ and $Gas6^{-/-}$ mice and analyzed by flow cytometry. Representative FACS plots and graphs demonstrate the frequencies of Treg cells and mean fluorescence intensity (MFI) of FOXP3 in Treg cells. Data represent the mean of five mice ± SEM. Representative data of one of two independent experiments are shown. (*G*) Cervical LN cells were collected from $Gas6^{+/+}$ and $Gas6^{-/-}$ mice, stimulated with PMA/ionomycin, and analyzed by ICS. Representative FACS plots and graphs demonstrate the frequencies of $IL\text{-}17A^+$ $CD4^+$ T cells, and the MFI of IL-17A in these cells. Data represent the mean of five mice ± SEM. Representative data of one of two independent experiments are shown.

found, suggesting that expression of GAS6 from two alleles might be required for maintaining microbial homeostasis (Fig. S3*A*). It should be mentioned that the microbial dysbiosis was not limited to the oral mucosa, as we also found an increase of total bacteria in feces of $Gas6^{-/-}$ mice accompanied by an expansion of certain bacterial families (Fig. S3 *B* and *C*).

To further verify the role of GAS6 in homeostatic regulation, we first cohoused $Gas6^{-/-}$ and $Gas6^{+/+}$ mice for 2 mo and examined whether this procedure alters their oral microbiota. As depicted in Fig. 6*A*, housing the mice in the same cage did not alter the load of oral microbiota either in $Gas6^{-/-}$ or $Gas6^{+/+}$ mice. Using specific primers to identify ribosomal 16S gene of distinct bacterial families, we verified that each group of mice maintained its original diversity of oral bacteria (Fig. 6*A*). We then analyzed the microbial and immunological status of $Gas6^{-/-}$ and $Gas6^{+/+}$ mice 2 wk after birth, a time at which GAS6 is not yet expressed in the oral epithelium. As demonstrated in Fig. 6*B*, the overall bacterial load in 2-wk-old mice was comparable in $Gas6^{-/-}$ and $Gas6^{+/+}$ mice, in contrast to adult mice. We also found that bacterial composition was similar in the oral cavities of 2-wk-old $Gas6^{+/+}$ and $Gas6^{-/-}$ mice but not in adult mice (Fig. 6*B*). We next quantified expression levels of TNF-α, IL-17A, FOXP3, and IL-10, which were differentially expressed in the oral mucosa of adult $Gas6^{-/-}$ and $Gas6^{+/+}$ mice (Fig. 3). Our analysis clearly indicated that these molecules were equally expressed in the oral mucosa of 2-wk-old mice of both groups of mice (Fig. 6*C* and Fig. S4). Collectively, our data suggest that expression of GAS6 induced by the oral microbiota a few weeks after birth is crucial to maintain microbial homeostasis.

Oral Bacteria Expanded in $Gas6^{-/-}$ Mice Are Capable of Using Nitrate Reactive Intermediates for Anaerobic Respiration. Because a large fraction of the expanded bacteria in $Gas6^{-/-}$ mice are known to use nitrate reactive intermediates for anaerobic respiration (18, 19), we hypothesized that the microbial dysbiosis observed in $Gas6^{-/-}$ mice might be related, in part, to the elevated inflammatory milieu found in their oral mucosa. By expressing enzymes such as nitrate reductase, these anaerobic bacteria can use electron acceptors generated as a byproduct of inflammation to support their growth by anaerobic respiration (18). To examine this hypothesis, we first quantified expression of three major enzymes *Doux2*, *Nos2* (iNOS), and *NOX1* induced in epithelial cells and neutrophils, which produce reactive oxygen (O_2^-) and nitrogen (NO^-) species. As depicted in Fig. 7*A*, higher expression levels of the noted enzymes were found in the oral mucosa of $Gas6^{-/-}$ compared with $Gas6^{+/+}$ mice. We next tested expression of nitrate reductase in RNA generated from oral bacterial samples and found significant higher expression levels of this enzyme in $Gas6^{-/-}$ mice (Fig. 7*B*). Analysis of the mouse saliva also revealed increased levels of nitrite (NO_2^-), the direct product of reduced NO_3^-, in $Gas6^{-/-}$ mice saliva samples compared with the $Gas6^{+/+}$ mice (Fig. 7*C*). Taken together, these results suggest that

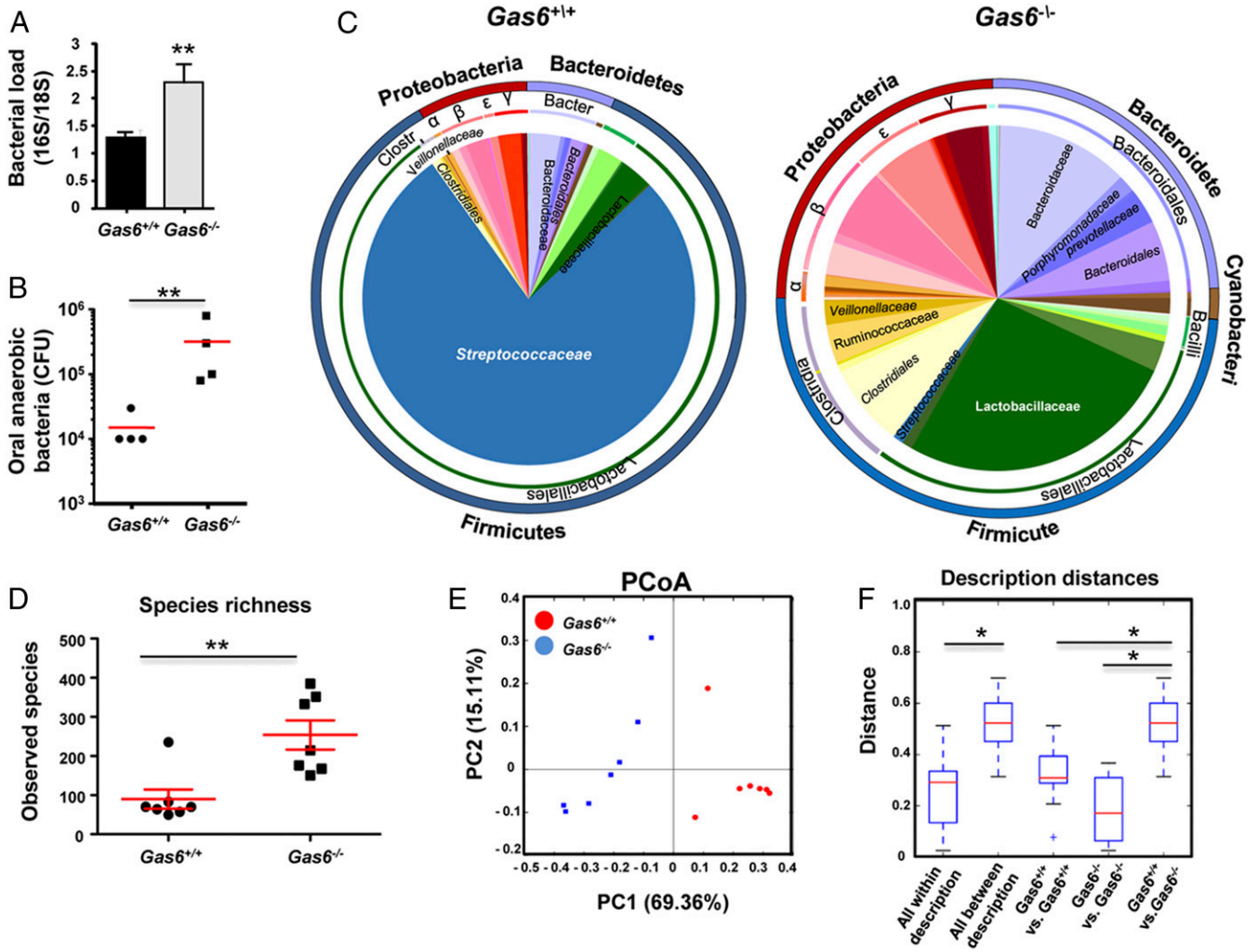

Fig. 5. Expansion of anaerobic bacteria in oral mucosa of *Gas6*$^{-/-}$ mice. (*A*) Total bacteria were enumerated in oral swabs taken from *Gas6*$^{-/-}$ and *Gas6*$^{+/+}$ littermate control mice by RT-qPCR of the 16S rRNA gene. Bar graphs present the 16S/18S ratio in each group and represent the mean values ± SEM (n = 6–10). (*B*) The oral cavities of *Gas6*$^{-/-}$ and B6 mice were sampled and plated on blood agar under anaerobic conditions. Cfu data of total cultivable oral anaerobic bacteria are shown for each individual mouse with horizontal lines denoting mean values. Representative data of one of three independent experiments are shown. (*C*) Relative abundance of taxa in oral swabs sampled from *Gas6*$^{+/+}$ and *Gas6*$^{-/-}$ mice. Pie charts represent the average distribution of sequences in operational taxonomic units (OTUs) assigned to each genus. (*D*) Alpha diversity plot representing taxa richness in samples of *Gas6*$^{+/+}$ and *Gas6*$^{-/-}$ mice. Data represent the mean of seven to eight mice ± SEM. (*E*) Principal coordinates analysis (PCoA) of weighted UniFrac distances based on 16S rRNA of *Gas6*$^{+/+}$ versus *Gas6*$^{-/-}$. (*F*) Box plot of distances described in *E*. Nonparametric *P* value of 0.01 (Bonferroni corrected) is presented as *. Representative taxonomic data of one of two independent experiments are shown.

the elevated production of reactive nitrate intermediates in the oral mucosa of *Gas6*$^{-/-}$ mice facilitates expansion of anaerobic bacteria expressing nitrate reductase for anaerobic respiration.

Expression of GAS6 in Epithelial Cells Rather than Hematopoietic Cells Shapes Oral Mucosal Homeostasis. We next sought to dissect the role of GAS6 expressed by epithelial cells versus hematopoietic cells such as DCs in maintaining oral homeostasis. For this step, we lethally irradiated CD45.2^{+} *Gas6*$^{-/-}$ and CD45.1^{+} B6 WT mice and reconstituted their immune system with BM purified from *Gas6*$^{-/-}$ or WT mice. Eight weeks later successful BM reconstitution was verified in the blood (Fig. S5*A*), and then microbial and immunological status of the mice were examined as described above. We first established that reconstitution of *Gas6*$^{-/-}$ (G) and WT (W) mice with their own BM cells (G→G and W→W, respectively) restored the microbial differences found in these mice without irradiation (Fig. 8 *A*–*C*). However, whereas reconstitution of WT mice with BM of *Gas6*$^{-/-}$ mice (G→W) had no impact on the load and diversity of oral microbiota, administration of WT BM cells into *Gas6*$^{-/-}$ mice (W→G) resulted in a significant alteration of the oral microbiota. However, the changes in the load and diversity of the oral microbiota in W→G were less than those observed in G→G mice, suggesting that, whereas only the absence of epithelial GAS6 enables microbial dysbiosis, its absence in hematopoietic cells further amplifies this process. Next, we examined immunological functions in the chimeric mice. Flow cytometry analysis revealed higher frequencies of neutrophils in G→G and W→G mice in comparison with the other two groups (Fig. 8*D* and Fig. S5*B*). However, the percentages of these cells in the oral mucosa of G→G mice were significantly higher than in W→G mice, in correlation to the level of microbial dysbiosis found in these groups. Using RT-qPCR analysis, we found an elevation in IL-17A and IFN-α expression, but a reduction in IL-10 and FOXP3 expression levels, in the oral mucosa of G→G and W→G mice compared with the other groups (Fig. 8*E*). With regards to FOXP3, flow cytometry analysis of the LN revealed reduced numbers of Treg cells, as well as lower FOXP3 expression per cell, only in mice in which GAS6

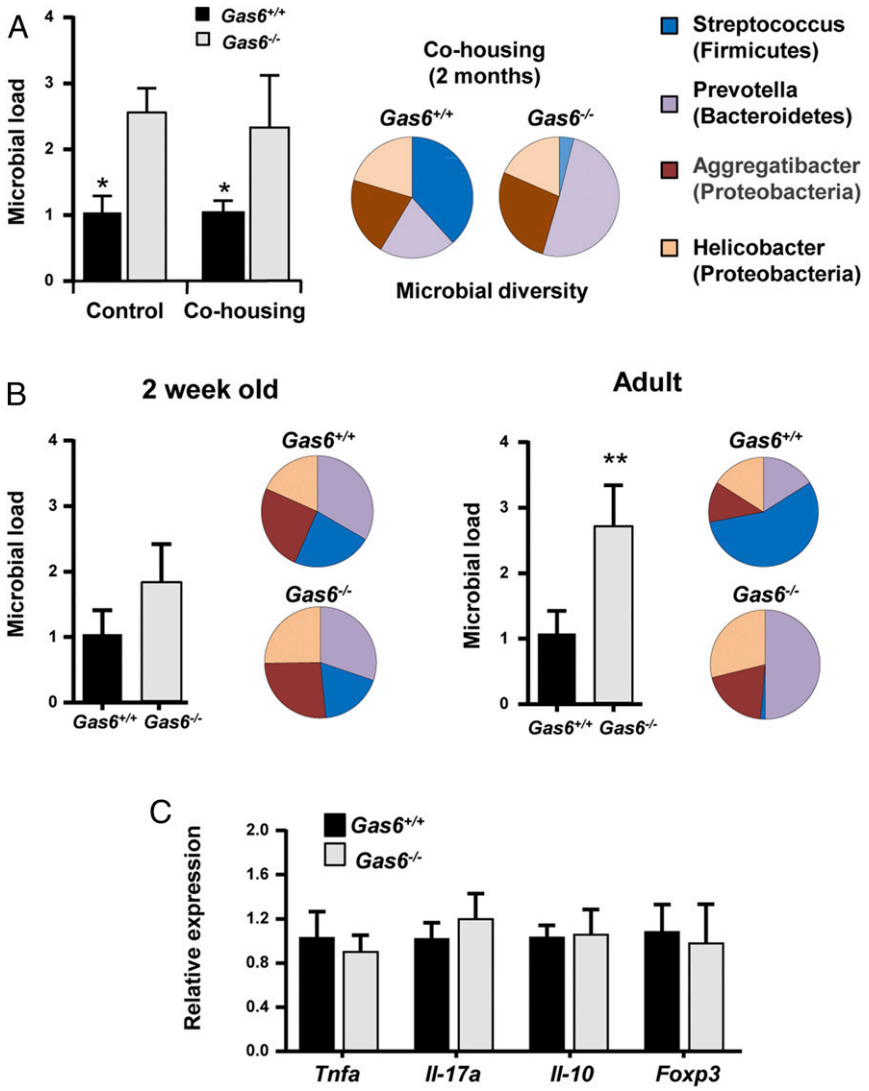

Fig. 6. The oral microbiota in *Gas6*$^{-/-}$ and *Gas6*$^{+/+}$ mice is terminally defined during maturation to adulthood and is not altered by cocaging. (*A*) Adult *Gas6*$^{-/-}$ and *Gas6*$^{+/+}$ mice were cohoused or housed separately. Two months later, oral swabs were taken from the mice to quantify total bacteria by RT-qPCR of the 16S rRNA gene. Bar graphs present the 16S/18S ratio in each group and represent the mean values of five mice ± SEM. To examine bacterial composition, the levels of certain bacterial families were quantified using specific primers for their ribosomal 16S genes. Pie charts represent the average relative frequency of each bacterial family examined. (*B*) Oral swabs were taken from 2-wk-old and adult (8 wk old) mice and total bacteria as well as the diversity of certain bacterial families were determined and presented as described above. (*C*) Bar graph depicts the relative mRNA levels of various immunological molecules in the gingiva of *Gas6*$^{+/+}$ and *Gas6*$^{-/-}$ mice using RT-qPCR and represents the mean of five mice ± SEM. Representative data of one of two independent experiments are shown.

was deleted in hematopoietic cells (G→G and G→W mice) (Fig. S5*C*). Whereas this suggests that the impairment in Treg activity is intrinsic to this cell compartment, its impact on the oral mucosa is predominantly determined by oral epithelial cells. In agreement with the capacity of epithelial cells to express *Duox2* and *Nox1*, the absence of GAS6 in the epithelium of G→G and W→G mice resulted in an overexpression of these molecules compared with WT recipient mice (Fig. 8*F*). Expression of iNOS (*Nos2*), however, which is expressed by both neutrophils and epithelial cells, was significantly up-regulated only in G→G mice, demonstrating the importance of GAS6 deletion in both hematopoietic and nonhematopoietic cells to this process. Finally, higher expression levels of *NapA* were found in G→G and W→G mice, as well as elevated nitrite levels, in line with the expansion of anaerobic bacteria observed in these mice (Fig. 8 *F*–*H*). Taken together, these data highlight the critical role of GAS6 in epithelial cells in maintaining oral homeostasis, whereas the absence of GAS6 in hematopoietic cells synergizes the level of dysbiosis.

***Gas6*$^{-/-}$ Mice Are Protected from Age-Associated Periodontitis Despite the Presence of Gingival Immunological and Microbial Dysbiosis.** It has been suggested that microbial dysbiosis can lead to an inflammation-driven bone loss, the hallmark of periodontitis (20). Moreover, commensal bacteria were also implicated in instigating age-associated periodontitis as they induce a low-grade chronic inflammation in the gingiva (20). Our results clearly demonstrate the presence of higher inflammatory response in the gingiva of *Gas6*$^{-/-}$ mice in comparison with *Gas6*$^{+/+}$ mice (Fig. 3). Consequently we studied the microbiota located in the gingiva that contains the dental biofilm, rather than examining the microbiota of the whole oral cavity obtained by oral swabs. Similar to what we described in the whole oral cavity samples, elevated bacterial load as well as altered diversity were found in gingiva of *Gas6*$^{-/-}$ mice in comparison with *Gas6*$^{+/+}$ mice (Fig. S6 *A*–*C*). Because the observed microbial and immunological dysbiosis is hypothesized to induce alveolar bone loss, we examined age-associated periodontitis in the gingiva of young (2–4 mo) versus aged (20–24 mo) *Gas6*$^{-/-}$ and *Gas6*$^{+/+}$ mice. First, we quantified gingival expression

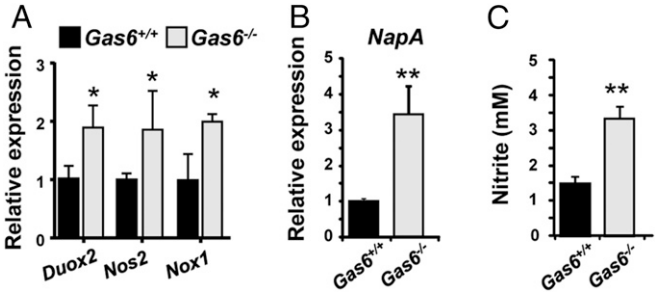

Fig. 7. Oral bacteria expanded in *Gas6*$^{-/-}$ mice are capable of using nitrate reactive intermediates for anaerobic respiration. (*A*) Quantification by RT-qPCR showing relative expression levels of *Duox2*, *Nos2*, and *Nox1* in the gingiva of *Gas6*$^{+/+}$ and *Gas6*$^{-/-}$ littermates. Data represent the mean of 5 mice ± SEM. (*B*) Relative expression levels of nitrate reductase *NapA* gene in RNA purified from bacterial samples obtained from *Gas6*$^{+/+}$ and *Gas6*$^{-/-}$ mice. Data represent the mean of 5 mice ± SEM. (*C*) Concentrations of nitrite (NO_2^-) in the saliva of *Gas6*$^{+/+}$ and *Gas6*$^{-/-}$ mice. Data represent the mean of 13 mice ± SEM. Representative data of one of two to three independent experiments are shown.

levels of receptor activator of nuclear factor κ B ligand (RANKL) and osteoprotegerin (OPG), critical regulators of osteoclastogenesis and bone resorption (21). Despite their immunological and microbial dysbiosis, RANKL and OPG levels were not significantly changed during aging in *Gas6*$^{-/-}$, whereas in *Gas6*$^{+/+}$ mice, increased RANKL expression and reduced OPG expression resulted in a reduced RANKL/OPG ratio that favors bone resorption (Fig. S6*E*) (21). Examining the alveolar bone morphology and quantifying residual alveolar bone confirmed these results, demonstrating considerable bone loss in aged *Gas6*$^{+/+}$ mice but not in aged *Gas6*$^{-/-}$ mice (Fig. S6 *E*–*G*). Whereas the lack of alveolar bone loss in aged *Gas6*$^{-/-}$ mice does not reflect the immunological and microbial status of their gingiva, it is in agreement with previous studies reporting that GAS6 is crucial for the resorption function of mature osteoclasts (22, 23). Therefore, although *Gas6*$^{-/-}$ mice should have an increased periodontal bone loss based on their periodontal immunological and microbial dysbiosis, the lack of Gas6 that prevents osteoclast function, ultimately, protects these mice from alveolar bone loss.

Discussion

In this study, we first demonstrated that GAS6 plays a fundamental role in maintaining oral mucosal homeostasis. Induction of GAS6 expression in epithelial cells by oral bacteria reduced steady-state antimicrobial immune responses, suggesting that GAS6 provokes epithelial changes, facilitating adaption to the developing microbiota (Fig. S7). The similar immunological and microbial status observed in 2-wk-old *Gas6*$^{-/-}$ and *Gas6*$^{+/+}$ mice, a period in which GAS6 is not normally expressed, further indicates the critical role of GAS6 in this process. Interestingly, PROS1 levels were unchanged, indicating that both TAM ligands are differentially regulated in this setting. The MYD88-dependent expression of GAS6 is likely to be induced via TLR signaling, because TAM molecules are known to be up-regulated upon TLR stimulation (24). Moreover, oral mucosal epithelial cells constitutively express TLR2 and TLR4, recognizing bacterial peptidoglycans and lipopolysaccharides, respectively (25). Nevertheless, despite the absolute dependence of GAS6 expression on oral microbiota, GAS6 was not expressed 1–3 wk after birth, a time in which bacteria are already present in the oral cavity. It is possible that alteration in the oral microbial load or composition occurring during the first few weeks after birth, presumably related to the weaning procedure or tooth eruption, stimulate GAS6 expression. An additional explanation could be postnatal developmental changes in the oral mucosa that are driven by commensals, similar to other mucosal sites (26). We have shown recently that Langerhans cells gradually populate the oral epithelium 2 mo after birth (27), thus supporting the idea of gradual maturation of the epithelium during this period. Such homeostatic innate and adaptive responses are critical to adjust the mucosa to meet environmental requirements, particularly during the transition from the protected fetal life to the intense postnatal interactions with oral commensals.

Our study demonstrates irrefutably the expression of GAS6 in freshly purified murine DCs. Expression of GAS6 by DCs enables tolerogenic immune responses to the microbiota by regulating IL-6 levels favoring the differentiation of Treg over Th17 cells in vivo. Such a GAS6-mediated reduction of IL-6 expression was previously reported in vitro using monocyte/macrophage cells (28). Of note, the absence of GAS6 not only reduced the frequencies of Treg cells, but also decreased FOXP3 expression levels on a per-cell basis. This finding suggests that the regulatory function of Treg cells was severely impaired in *Gas6*$^{-/-}$ mice (17). Nevertheless, the ability of GAS6 to modulate polarization of Treg/Th17 in DCs in vivo is instructed by signals initiated by epithelial cells, because the absence of Gas6 in hematopoietic cells alone (Gas6$^{-/-}$→ WT) had no significant impact on the mice. Previous studies have shown that Th17 and Treg cells play an important role in the development of experimental periodontitis (29, 30). It was also suggested that periodontitis could be a result of oral microbial dysbiosis induced by periodontal pathogens (20). Because we found that GAS6 expression is controlled by bacteria, it is tempting to hypothesize that oral pathogens might have the capacity to modulate GAS6 levels and by that to alter Th17/Treg balance, to induce microbial dysbiosis and subsequently periodontitis. Regardless of the precise mechanism, the direct impact of GAS6 on these two periodontitis-associated causes strongly suggests the involvement of GAS6 in periodontitis. Although the critical role of GAS6 on osteoclast function precludes an impact on the oral mucosa with periodontal bone loss, further studies developing novel cell-specific ablation of GAS6 might be able to show such connection.

The dysbiosis observed in our study is likely to be associated with both host–microbe and microbe–microbe interactions. The host inflammatory response developed in the absence of GAS6 probably eliminated certain bacteria, whereas the ability to use inflammation byproducts for anaerobic respiration facilitates the growth of others. A similar phenomenon was recently observed in the intestine at various experimental settings (31–33). Expansion of Proteobacteria in *Gas6*$^{-/-}$ mice correlates well with their superior capacity to produce nitrate reductase (18). Such activity might also explain the striking shift from *Streptococcaceae* to *Lactobacillaceae* within the Firmicutes phylum, as the latter are also capable of denitrification, which could be used for anaerobic respiration (19). Augmentation of the Bacteroidetes phylum in the oral mucosa of *Gas6*$^{-/-}$ mice, particularly the *Porphyromonadaceae* and *Prevotellaceae* families, is highly relevant to oral health. These populations include several key oral pathogens such as *Porphyromonas gingivalis*, *Prevotella intermedia*, *and Tannerella forsythia* that flourish in periodontal inflammation and are closely associated with tissue destruction (34).

As a ligand of the TAM signaling system, GAS6 is expressed by many cell types and could act on its receptors either locally or remotely (9). We demonstrate in this work that GAS6 and its potent receptor AXL are expressed by epithelial cells as well as DCs. The results obtained by the chimeric mice experiments suggest that GAS6 is likely to act in an autocrine/paracrine fashion on epithelial cells. With regard to DCs, the higher expression of IL-6 by these cells upon stimulation in vitro suggests that GAS6 can also act in an autocrine/paracrine fashion on DCs, but this might not accurately reflect the situation in vivo. Indeed, the precise mechanisms by which TAM ligands engage their receptors are not fully understood, and further investigation is required to address this issue.

In summary, this study reveals a critical role for epithelial GAS6 in regulating host–commensal homeostatic interactions in the murine oral mucosa. The similarity in the pattern of GAS6 and PROS1 expression among mouse and human gingival tissues

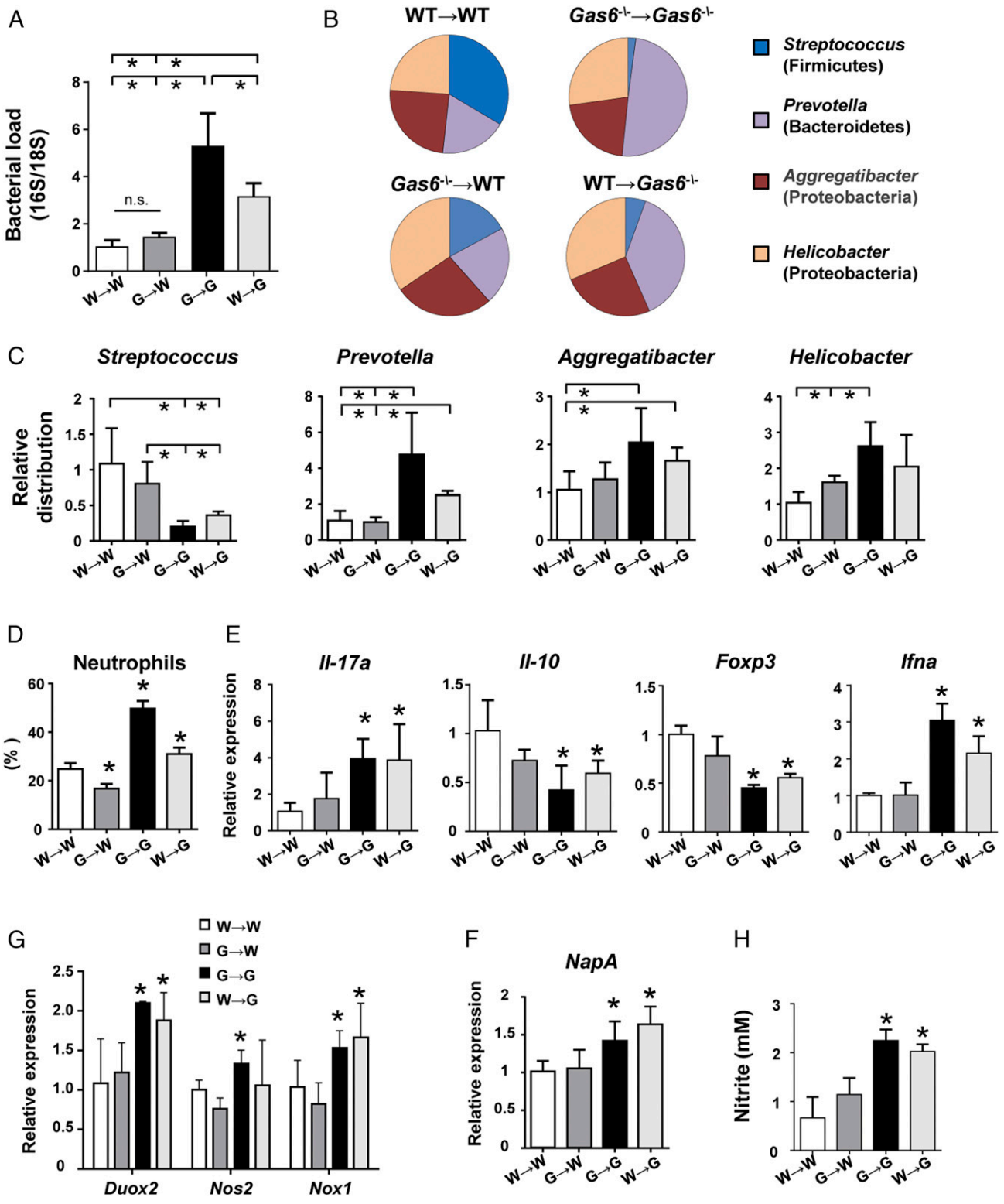

Fig. 8. GAS6 expressed by epithelial cells rather than by hematopoietic cells controls oral mucosal homeostasis. CD45.2$^+$ *Gas6*$^{-/-}$ and CD45.1$^+$ WT B6 mice were lethally irradiated and 24 h later received BM purified from either CD45.2$^+$ *Gas6*$^{-/-}$ or CD45.1$^+$ WT B6 mice. Eight weeks after bone marrow reconstitution, the mice were analyzed. (*A*) Oral swabs were taken from the mice to quantify total bacteria by RT-qPCR. Bar graphs present the 16S/18S ratio in each group and represent the mean values of three mice ± SEM. Diversity of certain bacterial families was quantified using specific primers for their ribosomal 16S genes. (*B*) Pie charts represent the average relative frequency of each bacterial family examined. (*C*) Bar graphs present the relative distribution of each bacterial family among the various groups of irradiated mice. (*D*) Frequencies of neutrophils in the oral mucosa as determined by flow cytometry. (*E*) Quantification by RT-qPCR the mRNA levels of *Il-17a*, *Il-10*, *Foxp3*, and *Ifna* in the gingiva. (*F*) Quantification by RT-qPCR the relative expression levels of *Duox2*, *Nos2*, and *Nox1* in the gingiva. (*G*) Relative expression levels of nitrate reductase *NapA* gene in RNA purified from bacterial samples obtained from the mice. (*H*) Concentrations of nitrite (NO_2^-) in the saliva of the chimeric mice. Data represent the mean of three mice ± SEM. Representative data of one of two independent experiments are shown. n.s., no statistical significance; W, WT; G, *Gas6*$^{-/-}$.

strongly suggest a role for TAM signaling in maintaining oral mucosal homeostasis also in human. The present data thus expand our capacity to understand oral diseases, which might facilitate the development of novel therapeutic strategies.

Experimental Procedures

Mice. C57BL/6JOlaHsd (B6) were purchased from Harlan. *Gas6*$^{-/-}$ mice were kindly provided by Greg Lemke, Salk Institute, La Jolla, CA. For most of the studies described in this work littermate controls of *Gas6*$^{+/+}$ and *Gas6*$^{-/-}$ mice were used. All animal protocols were approved by the Hebrew University Institutional Animal Care and Ethics Committee. Germ-free (GF) or SPF adult male outbred Swiss Webster mice (a widely used mouse strain in GF experiments) were maintained in sterile isolators at the Weizmann Institute. For cohousing experiments GF mice were housed with SPF mates for 2 mo. All GF studies were approved by the Institutional Animal Care and Use Committee of the Weizmann Institute of Science. The identity of the mice used for experiments is described in *SI Materials and Methods*.

Antibodies and Reagents. Antibodies and reagents are described in *SI Materials and Methods*.

Immunofluorescence Staining. The murine maxilla was treated as described in *SI Materials and Methods*. Staining of human gingival cross-section was performed on freshly isolated tissues as described above, under the approval obtained by the Hadassah Medical Center Institutional Review Board. Informed consent was provided in accordance with the Declaration of Helsinki.

RNA Extraction and Real-Time PCR. For RNA isolation the maxilla was homogenized in 1 mL TRI reagent (Sigma) using an electric homogenizer, and RNA was extracted as described in *SI Materials and Methods*. Sequences of primers that were used for RT-qPCR are listed in Table S1.

Analysis of T Cells in the LNs. Cervical LNs were collected from *Gas6*$^{+/+}$ or *Gas6*$^{-/-}$ mice and treated as explained in *SI Materials and Methods*.

Isolation and Processing of Gingival Tissue. Gingival and skin cells were isolated as explained in *SI Materials and Methods*.

Preparation and Simulation of BMDCs. BMDCs were prepared and stimulated as described in *SI Materials and Methods*.

Cultivation of Oral Microbiota. Oral cavity of anesthetized individual *Gas6*$^{+/+}$ or *Gas6*$^{-/-}$ littermate control mice were swabbed for 30 s and the swabs were then inserted into Eppendorf tubes containing 100 μL of Wilkins-Chalgren medium (Oxoid). The samples were serially diluted and plated on blood agar for 2 d under anaerobic conditions at 37 °C and colonies were enumerated to determine the colony-forming units (cfus) of total cultivatable oral anaerobic bacteria.

In Vivo BM Reconstitution Assays. Eight-week-old recipient CD45.2^{+} *Gas6*$^{-/-}$ or CD45.1^{+} B6 mice were lethally irradiated with 950 rad and 24 h later the mice were injected i.v. with 5×10^6 BM cells obtained from either congenic CD45.2^{+} *Gas6*$^{-/-}$ or CD45.1^{+} B6 mice to allow identification of donor-derived cells. The chimerism was verified in the blood as indicated in the text.

Western Blot. Gingival tissues were isolated and homogenized in ice-cold lysis buffer (50 mM Tris pH 7.5, 150 mM NaCl, 1% Triton X-100, 0.5% Nonidet P-40, 0.1% SDS, 0.5 mM EDTA) supplemented with a protease inhibitor mixture (Sigma). Following lysate incubation for 30 min on ice, tissue debris were removed by centrifugation as described in *SI Materials and Methods*.

Taxonomic Microbiota Analysis. For 16S amplicon pyrosequencing, PCR amplification was performed spanning the V1/2 region of the 16S rRNA gene and subsequently sequenced using 500-bp paired-end sequencing (Illumina MiSeq). Reads were then processed using the QIIME (quantitative insights into microbial ecology) analysis pipeline with USEARCH against the Greengenes Database.

Statistical Analysis. Data were expressed as means ± SEM. Statistical tests were performed using one-way analysis of variance (ANOVA) and Student's *t* test. $P < 0.05$ was considered significant. $^{*}P < 0.05$; $^{**}P < 0.01$.

ACKNOWLEDGMENTS. This work was supported by United States–Israel Binational Science Foundation Grant 2015209 (to A.-H.H.), and Israel Science Foundation Grant 1764/12 (to T.B.-C.).

1. Kagnoff MF (2014) The intestinal epithelium is an integral component of a communications network. *J Clin Invest* 124(7):2841–2843.
2. Whitsett JA, Alenghat T (2015) Respiratory epithelial cells orchestrate pulmonary innate immunity. *Nat Immunol* 16(1):27–35.
3. Eskan MA, et al. (2008) TLR4 and S1P receptors cooperate to enhance inflammatory cytokine production in human gingival epithelial cells. *Eur J Immunol* 38(4): 1138–1147.
4. Greer A, Zenobia C, Darveau RP (2013) Defensins and LL-37: A review of function in the gingival epithelium. *Periodontol 2000* 63(1):67–79.
5. Kolenbrander PE, Palmer RJ, Jr, Periasamy S, Jakubovics NS (2010) Oral multispecies biofilm development and the key role of cell-cell distance. *Nat Rev Microbiol* 8(7): 471–480.
6. Hajishengallis G (2015) Periodontitis: From microbial immune subversion to systemic inflammation. *Nat Rev Immunol* 15(1):30–44.
7. Rothlin CV, Carrera-Silva EA, Bosurgi L, Ghosh S (2015) TAM receptor signaling in immune homeostasis. *Annu Rev Immunol* 33:355–391.
8. Lemke G, Burstyn-Cohen T (2010) TAM receptors and the clearance of apoptotic cells. *Ann N Y Acad Sci* 1209:23–29.
9. Lemke G, Rothlin CV (2008) Immunobiology of the TAM receptors. *Nat Rev Immunol* 8(5):327–336.
10. van der Meer JH, van der Poll T, van 't Veer C (2014) TAM receptors, Gas6, and protein S: Roles in inflammation and hemostasis. *Blood* 123(16):2460–2469.
11. Burstyn-Cohen T, et al. (2012) Genetic dissection of TAM receptor-ligand interaction in retinal pigment epithelial cell phagocytosis. *Neuron* 76(6):1123–1132.
12. Burstyn-Cohen T, Heeb MJ, Lemke G (2009) Lack of protein S in mice causes embryonic lethal coagulopathy and vascular dysgenesis. *J Clin Invest* 119(10):2942–2953.
13. Nagata K, et al. (1996) Identification of the product of growth arrest-specific gene 6 as a common ligand for Axl, Sky, and Mer receptor tyrosine kinases. *J Biol Chem* 271(47):30022–30027.
14. Rodrigue L, Barras MJ, Marcotte H, Lavoie MC (1993) Bacterial colonization of the oral cavity of the BALB/c mouse. *Microb Ecol* 26(3):267–275.
15. Littman DR, Rudensky AY (2010) Th17 and regulatory T cells in mediating and restraining inflammation. *Cell* 140(6):845–858.
16. Gough DJ, Messina NL, Clarke CJ, Johnstone RW, Levy DE (2012) Constitutive type I interferon modulates homeostatic balance through tonic signaling. *Immunity* 36(2): 166–174.
17. Wan YY, Flavell RA (2007) Regulatory T-cell functions are subverted and converted owing to attenuated Foxp3 expression. *Nature* 445(7129):766–770.
18. Winter SE, Bäumler AJ (2014) Dysbiosis in the inflamed intestine: Chance favors the prepared microbe. *Gut Microbes* 5(1):71–73.
19. Xu J, Verstraete W (2001) Evaluation of nitric oxide production by lactobacilli. *Appl Microbiol Biotechnol* 56(3–4):504–507.
20. Hajishengallis G, et al. (2011) Low-abundance biofilm species orchestrates inflammatory periodontal disease through the commensal microbiota and complement. *Cell Host Microbe* 10(5):497–506.
21. Cochran DL (2008) Inflammation and bone loss in periodontal disease. *J Periodontol* 79(8, Suppl):1569–1576.
22. Katagiri M, et al. (2001) Mechanism of stimulation of osteoclastic bone resorption through Gas6/Tyro 3, a receptor tyrosine kinase signaling, in mouse osteoclasts. *J Biol Chem* 276(10):7376–7382.
23. Nakamura YS, et al. (1998) Tyro 3 receptor tyrosine kinase and its ligand, Gas6, stimulate the function of osteoclasts. *Stem Cells* 16(3):229–238.
24. Rothlin CV, Ghosh S, Zuniga EI, Oldstone MB, Lemke G (2007) TAM receptors are pleiotropic inhibitors of the innate immune response. *Cell* 131(6):1124–1136.
25. Sugawara Y, et al. (2006) Toll-like receptors, NOD1, and NOD2 in oral epithelial cells. *J Dent Res* 85(6):524–529.
26. Fulde M, Hornef MW (2014) Maturation of the enteric mucosal innate immune system during the postnatal period. *Immunol Rev* 260(1):21–34.
27. Capucha T, et al. (2015) Distinct murine mucosal Langerhans cell subsets develop from pre-dendritic cells and monocytes. *Immunity* 43(2):369–381.
28. Alciato F, Sainaghi PP, Sola D, Castello L, Avanzi GC (2010) TNF-alpha, IL-6, and IL-1 expression is inhibited by GAS6 in monocytes/macrophages. *J Leukoc Biol* 87(5): 869–875.
29. Arizon M, et al. (2012) Langerhans cells down-regulate inflammation-driven alveolar bone loss. *Proc Natl Acad Sci USA* 109(18):7043–7048.
30. Gaffen SL, Hajishengallis G (2008) A new inflammatory cytokine on the block: Rethinking periodontal disease and the Th1/Th2 paradigm in the context of Th17 cells and IL-17. *J Dent Res* 87(9):817–828.
31. Winter SE, et al. (2010) Gut inflammation provides a respiratory electron acceptor for Salmonella. *Nature* 467(7314):426–429.
32. Winter SE, et al. (2013) Host-derived nitrate boosts growth of E. coli in the inflamed gut. *Science* 339(6120):708–711.
33. Smith PM, et al. (2013) The microbial metabolites, short-chain fatty acids, regulate colonic Treg cell homeostasis. *Science* 341(6145):569–573.
34. Socransky SS, Haffajee AD, Cugini MA, Smith C, Kent RL, Jr (1998) Microbial complexes in subgingival plaque. *J Clin Periodontol* 25(2):134–144.